Journal of Biomedical Optics

BiomedicalOptics.SPIEDigitalLibrary.org

Correlation between electrical and hemodynamic responses during visual stimulation with graded contrasts

Juanning Si
Xin Zhang
Yuejun Li
Yujin Zhang
Nianming Zuo
Tianzi Jiang

SPIE.

Juanning Si, Xin Zhang, Yuejun Li, Yujin Zhang, Nianming Zuo, Tianzi Jiang, "Correlation between electrical and hemodynamic responses during visual stimulation with graded contrasts," *J. Biomed. Opt.* **21**(9), 091315 (2016), doi: 10.1117/1.JBO.21.9.091315.

Correlation between electrical and hemodynamic responses during visual stimulation with graded contrasts

Juanning Si,[a,b,*] Xin Zhang,[a,b] Yuejun Li,[c] Yujin Zhang,[a,b] Nianming Zuo,[a,b] and Tianzi Jiang[a,b,c,d,e,*]
[a]Chinese Academy of Sciences, Brainnetome Center, Institute of Automation, Beijing 100190, China
[b]Chinese Academy of Sciences, National Laboratory of Pattern Recognition, Institute of Automation, Beijing 100190, China
[c]University of Electronic Science and Technology of China, Key Laboratory for NeuroInformation of the Ministry of Education, School of Life Science and Technology, Chengdu 625014, China
[d]Chinese Academy of Sciences, CAS Center for Excellence in Brain Science, Institute of Automation, Beijing 100190, China
[e]University of Queensland, Queensland Brain Institute, St. Lucia, Queensland 4072, Australia

Abstract. Brain functional activity involves complex cellular, metabolic, and vascular chain reactions, making it difficult to comprehend. Electroencephalography (EEG) and functional near infrared spectroscopy (fNIRS) have been combined into a multimodal neuroimaging method that captures both electrophysiological and hemodynamic information to explore the spatiotemporal characteristics of brain activity. Because of the significance of visually evoked functional activity in clinical applications, numerous studies have explored the amplitude of the visual evoked potential (VEP) to clarify its relationship with the hemodynamic response. However, relatively few studies have investigated the influence of latency, which has been frequently used to diagnose visual diseases, on the hemodynamic response. Moreover, because the latency and the amplitude of VEPs have different roles in coding visual information, investigating the relationship between latency and the hemodynamic response should be helpful. In this study, checkerboard reversal tasks with graded contrasts were used to evoke visual functional activity. Both EEG and fNIRS were employed to investigate the relationship between neuronal electrophysiological activities and the hemodynamic responses. The VEP amplitudes were linearly correlated with the hemodynamic response, but the VEP latency showed a negative linear correlation with the hemodynamic response. [DOI: 10.1117/1.JBO.21.9.091315]

Keywords: electroencephalography; functional near infrared spectroscopy; visual evoked potential; visual; contrast; latency.

Paper 150880SSRR received Dec. 31, 2015; accepted for publication Jul. 13, 2016; published online Aug. 5, 2016.

1 Introduction

The brain's functional activity involves neuronal electrophysiological signal transmission, chemical transmitter release, energy metabolism, and blood microcirculation.[1] These complex and serial cellular, metabolic, and vascular processes make it difficult to fully comprehend the functional activity of the brain. Nevertheless, neuroscientists have continued to investigate it and have attempted to resolve these processes one by one. Electrophysiology was the initial tool for exploring brain functional activity. Electroencephalography (EEG), a noninvasive, electrophysiological tool, has been utilized to measure electrical potentials on the scalp that originate from neuronal activity in the brain. This technique provided good submillisecond temporal resolution but relatively low spatial resolution.[2,3] Functional magnetic resonance imaging (fMRI) was found to indirectly reflect neuronal activity by measuring blood-oxygen-level dependent (BOLD) signals.[4] Numerous studies have used it to investigate vascular functional activity. BOLD signals measure changes in the paramagnetic properties of the deoxygenated hemodynamic content of tissue at a spatial resolution of tens of mm^3, but its temporal resolution has remained at a timescale of seconds.[5] Because the brain's functional activity is not limited to fluctuations in one type of physiological signal, EEG and fMRI have been combined to record signals originating from neuronal activity and microcirculation[6] even in certain brain disorders.[7] This combination seems to be appropriate for analyzing the two processes of the functional activity of the brain. However, serious cross interference between the electrical field of an EEG system and the magnetic field of an fMRI scanner has limited this combination as a multimodal tool for exploring brain activity with the expected precision.[8]

Jobsis[9] found that skull transparency and cerebral absorption of near infrared light allowed a noninvasive way to measure tissue oxygen properties. This finding, termed functional near infrared spectroscopy (fNIRS), provided an important optical technique for neuroscience. fNIRS reveals brain activity through the hemodynamic responses associated with neuronal activity. It is analogous to fMRI in that, in both of them, brain blood oxygen serves as an intermediate to indicate neuronal activity. Unlike fMRI, however, fNIRS reveals not only deoxygenated but also oxygenated and total hemoglobin concentrations. This allows fNIRS users to distinguish differences in the amplitude, timing, and location of these components at a high level of resolution that is comparable to that of EEG.[10–12] The combination of EEG and fNIRS has been utilized as a multimodal neuroimaging method in a variety of applications, such as brain

*Address all correspondence to: Juanning Si, E-mail: sijuanning@gmail.com; Tianzi Jiang, E-mail: jiangtz@nlpr.ia.ac.cns

1083-3668/2016/$25.00 © 2016 SPIE

computer interfaces,[10,13] the diagnosis of brain diseases,[3,14] and investigations into the functional activities of the brain.[15,16]

Visual evoked potentials (VEPs) are electrophysiological signals evoked by visual stimuli that can be extracted from the electroencephalographic activity in the visual cortex recorded from the overlying scalp.[17] VEPs, which have two critical parameters: amplitude and latency, can provide important diagnostic information about the functional integrity of the visual system.[17,18] The amplitude represents the amount of information received by the visual cortex, whereas the latency indicates how long the electrical signal took to travel from the retina to the visual cortex.[18] VEPs have been used to assess the vision of infants and young children since the 1970s.[19] Because of its value in clinical applications, many studies of VEPs have been conducted since that time to evaluate the visual pathway and to diagnose visual diseases.[18,20,21] Moreover, quite a few studies of the amplitude of VEPs have been performed to clarify its relationship with the hemodynamic response in order to investigate the so-called "neurovascular coupling" relationship.[22–32] To the best of our knowledge, most of these studies were conducted to determine the relationship between the amplitude and the hemodynamic response.

However, the number of studies that investigated the influence of the temporal characteristics (the latency) of the VEPs on the hemodynamic response is relatively small. In response to a given stimulus, millions of pyramidal neurons receive synchronized postsynaptic potentials to generate the corresponding response. As a result, it takes time for the input neurons to become synchronized.[33,34] Because EEG signals are thought to measure the synchronization above a certain threshold, these signals indicate changes in both onset and peak response latencies.[33] The more rapidly neurons become synchronized, the shorter the response latency. In general, the response latencies to visual stimuli are variable; i.e., distinct latencies correspond to distinct stimuli. A strong stimulus typically produces greater amplitudes and shorter latencies.[35,36] Differences in the latency-contrast relationship between different cells means that the signals will become increasingly asynchronous as the stimulus contrast is reduced.[37] In comparison, hemodynamic responses are thought to reflect increases in synaptic activities regardless of the level of synchronization between them.[34] The amplitude of VEPs is modulated by the strength of the stimulus, whereas their latency is more a function of stimulus contrast.[38,39] Some information is carried by the response latency because the stimulus contrast influences the response latency more than the response amplitude; that is to say, the stimulus contrast is encoded primarily by the response latency; whereas, the stimulus identity is encoded primarily by the response magnitude.[37] Temporal coding is important for distinguishing subtle contrast differences, while firing rates are useful for gross discrimination.[40] Therefore, clarifying the relationship between the latency and hemodynamic response is important.

Stimulus contrast, an important characteristic of the visual world, has been reported to offer several advantages as a paradigm for studying the ways in which information is encoded into the responses of neurons in the visual cortex.[40] Therefore, in this study, checkerboard reversal tasks with graded contrasts were used, and both EEG and fNIRS were employed to more comprehensively investigate the relationship between the electrophysiological activities of neurons and hemodynamic responses. The research goals were threefold. The first was to observe how a distinct contrast stimulus would affect the VEP and the hemodynamic response. The second was to correlate the VEP amplitude with the hemodynamic responses to explore the relationship between them. The last, but not least, was to investigate the effect of VEP latency on the hemodynamic response.

2 Materials and Methods

2.1 *Participants and Protocol*

Thirteen healthy volunteers (11 males and 2 females, ages 22 to 44 years) were recruited for this study. All the participants had normal or corrected-to-normal vision, no history of neurological disorders, and were not taking any type of medication at the time of the experiment. The visual stimuli we used were full-field windmill checkerboard reversal designs with three different levels of contrast (100%, 10%, and 1%). The stimulus contrast (C) was defined according to $C = (L_{\max} - L_{\min})/(L_{\max} + L_{\min})$, where $L_{\max}$ and $L_{\min}$ are the maximum and minimum luminances, respectively.[37] The order in which the different contrast levels were presented in the trials was randomized among the participants. For each contrast, the entire experimental protocol consisted of an initial baseline period (30 s) followed by seven blocks; each block consisted of a stimulation period (25 s in a block at a reversal frequency rate of 4 Hz) and a resting period (30 s). We set 4 Hz as the reversal frequency, because that rate can induce a strong and stable response while, on the other hand, avoiding the overlap between consecutive VEP waveforms.[29,41,42]

The complete protocol for each contrast lasted 415 s. During the baseline and resting periods, the participants were instructed to look at a central cross. During the stimulation periods, a full-field windmill checkerboard stimulus was presented. After each complete contrast session, the participants were allowed to take a break for several minutes to prevent them from becoming fatigued. The experimental protocol was approved by the ethics committee of the Institute of Automation, Chinese Academy of Sciences. Written informed consent was obtained, and a reward was given to each participant for participation. All the experiments were carried out in a quiet, dimly illuminated, acoustically shielded room. Before the formal measurement session, the experiment protocol was explained in detail to the participants, and they were trained until they were familiar with the paradigm. During the experiment, the participants were seated comfortably 80 cm in front of a computer monitor. All experimental stimuli were presented using E-prime 2.0 software. EEG and fNIRS were used to record the neuronal electrophysiological signals and vascular microcirculation, respectively. The experimental configuration is EEG as shown in Fig. 1.

2.2 *Electroencephalography Recording and Data Analysis*

VEPs were recorded using the Brain Vision system (Brain Products Ltd., Munich, Germany) with 64 channels at a sampling rate of 5000 Hz. Electrodes were placed at O1, O2, and Oz based on the international 10 to 20 system of electrode placement. An electrooculographic (EOG) electrode was placed over the outer canthus of the left eye to correct for blink artifacts. The impedances of the electrodes were maintained below 10 kΩ.

Prior to the correlation analysis, the EEG and fNIRS data were analyzed separately. Brain Vision Analyzer 2.0 was used for the off-line analysis of the EEG data. First, the O1, O2, Oz,

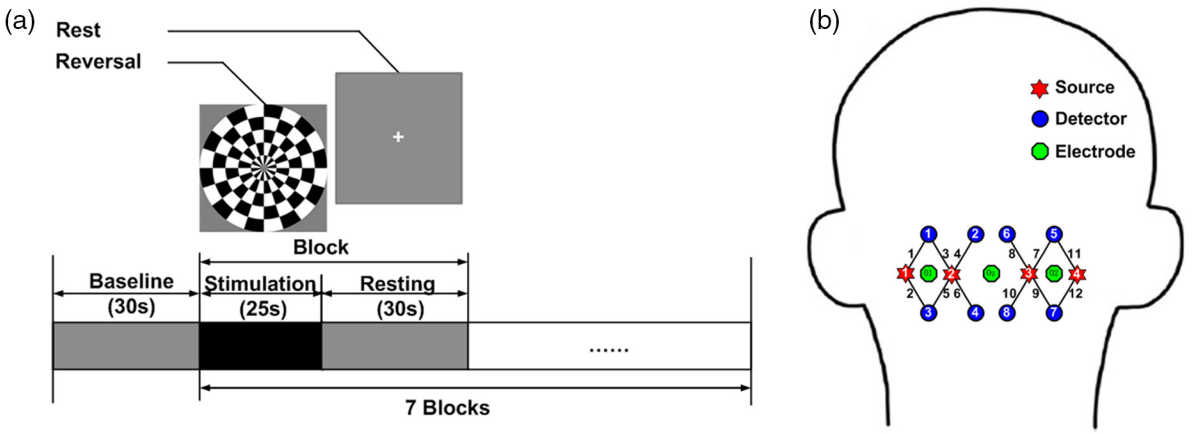

Fig. 1 Experimental configuration. (a) Experimental paradigm of the visual checkerboard reversal task. The entire experimental paradigm consisted of an initial baseline period (30 s) followed by seven blocks, each block consisted of a stimulation period (25 s, reversal frequency: 4 Hz) and a resting period (30 s). (b) The diagram of the head illustrates the placement of the electrodes (green hexagons), specifically, O1, O2, and Oz, and optodes, specifically 4 sources (red stars) and 8 detectors (blue circles), yielding 12 optical channels (black lines marked with channel numbers). The distance between a neighboring source and the detector pairs was 3 cm and the probe covered an area of $\sim 6 \times 6$ cm^2 for each hemisphere.

and EOG channels were selected for further processing. Then the data were down-sampled to 1000 Hz and band-filtered between 1 and 100 Hz with an additional 50 Hz notch filter. Moreover, an ocular correction using independent component analysis was done for the data that was seriously affected by EOG artifacts. Then the trend was subtracted from the data, taking into account the DC offset. The data were segmented into epochs that started 50 ms before the stimulus onset and ended 200 ms after the stimulus. Epochs with a magnitude greater than ± 50 μV were automatically rejected as artifacts. Finally, the data went through a baseline correction by subtracting the 50 ms baseline obtained prior to the stimulus marker, and the block averages were calculated.

2.3 *Functional Near Infrared Spectroscopy Recording and Data Analysis*

Hemodynamic responses were recorded using the TechEn CW6 system. Optodes were placed on the surface above the primary visual cortex guided by the O1, O2, and Oz electrode positions. Four sources and eight detectors were arranged geometrically to obtain 12 optical channels, as shown in Fig. 1. The distance between the source and detector pairs was 3 cm and the probe covered an area $\sim 6 \times 6$ cm^2 for each hemisphere. The sampling rate for the fNIRS was 50 Hz. In the optical recordings from the region of the visual cortex, the signals detected from the optical fibers of the CW6 system were especially weak. There may be two possible explanations for this. First, the relatively large tips of the fibers may have covered some of the participants' hair. Second, the coupling efficiency between the scalp and the optodes may have been poor because of the uneven structure of the occipital area. Therefore, we used self-designed fibers with smaller tips to obtain improved signal quality.

Data processing was conducted using Homer 2. First, the concentration changes of oxygenated (HbO), deoxygenated (Hb), and total (HbT) hemoglobin were calculated from the original raw data using the modified Beer-Lambert Law.[43,44] Next, the data were band-pass filtered between 0.01 and 0.1 Hz to remove higher frequency instrumental noise and task-unrelated physiological noise, including those from breathing, Mayer waves, blood pressure, arterial pulse oscillations, and heart beats at lower frequencies.[45,46] The differential pathlength factors were 6.51 and 5.86 for 690 and 830 nm, respectively.[47,48] The data were then segmented into epochs, starting 5 s before the activation onset and ending 20 s after the activation, and epochs with apparent artifacts were rejected. The 5 s period before the activation onset was regarded as the baseline. As is typical in other studies, a reliable brain activation was identified as a significant increase in ΔHbO or a significant decrease in ΔHb with respect to the average baseline levels between 8 s and 20 s after the activation onset.[46,49] The spatial distribution maps of the group-averaged hemodynamic responses were calculated for all the included data.

2.4 *Correlation Analysis and Statistical Analysis*

Throughout the experiment, reliable VEP waveforms from the EEG were obtained from all 13 participants, but reliable hemodynamic responses from the brain activation were obtained from fNIRS in 10 out of 13 participants. All data from three participants were discarded because of inadequate fNIRS recordings. One participant's data was rejected because he did not have an fNIRS scan. Another was rejected for poor optical coupling between the optodes and the scalp. The third one was removed due to unusually large motion artifacts. Therefore, the data from the remaining 10 participants were used in the subsequent data processing and analysis. For the fNIRS data, the trial rejection rates were 6.59%, 5.49%, and 3.3% for contrast levels 100%, 10%, and 1%, respectively. For the EEG data, the trial rejection rates were 10.32%, 9.51%, and 10.48% for contrast levels 100%, 10%, and 1%, respectively.

When comparing VEPs and hemodynamic responses, an important issue is which features of the VEPs should be used to represent the neuronal activity.[50] Previous papers used the first positive P1 peak for latency analysis because of its relatively good stability and high amplitude.[18,51,52] In this paper,

the amplitudes and latencies of the first negative N1 peak and the first positive P1 peak (because they were the most prominent peaks, whereas N2 could not be extracted consistently) were used to thoroughly investigate the relationship between the VEP and the hemodynamic responses. In this paper, all the experimental results are indicated as means ±SE, unless otherwise mentioned. A paired t-test was conducted to compare the differences in three contrast levels of VEPs and the hemodynamic responses, separately. The differences were accepted as significant when $p < 0.05$. All the statistical analyses were performed using SPSS software.

3 Results

3.1 *Electroencephalography Results*

The group-averaged VEP results for the different contrast levels in the checkerboard reversal experiment were extracted (Fig. 2). This figure shows that the records from the 100% contrast level indicated a typical pattern reversal VEP, including the first negative peak (N1, at about 75 ms) and the first positive peak (P1, at about 100 ms). The amplitudes of the P1 and N1 peaks for the 10% and 1% contrast levels were obviously reduced and the latencies were noticeably prolonged.

The group-averaged mean VEPs across O1, Oz, and O2 are shown in Fig. 3. The individual VEP data for the visual checkerboard reversal tasks at the different contrast levels are shown in Fig. 4. As Figs. 2 and 3 show, both the amplitude and the latency of the VEPs varied with stimulus contrast; specifically, a decrease in the contrast level caused a reduction in the amplitude and an increase in the latency of the VEPs. To test whether these changing trends were statistically significant (paired t-test, $p < 0.05$), we compared the three contrast levels with each other. As can be seen in Table 1, the amplitudes of P1–N1 were significantly different between the three contrast levels. As for the amplitudes of the P1, the 1% contrast result was statistically different from the 10% contrast and the 100% contrast, but there was no significant difference between 10% and the 100% contrast levels. Note that the P1 latencies were significantly different between all three contrast levels, but there were no significant differences in the N1 latencies between the three contrast levels. As shown in Fig. 4, the VEPs had a relatively high degree of intersubject variability in amplitude,

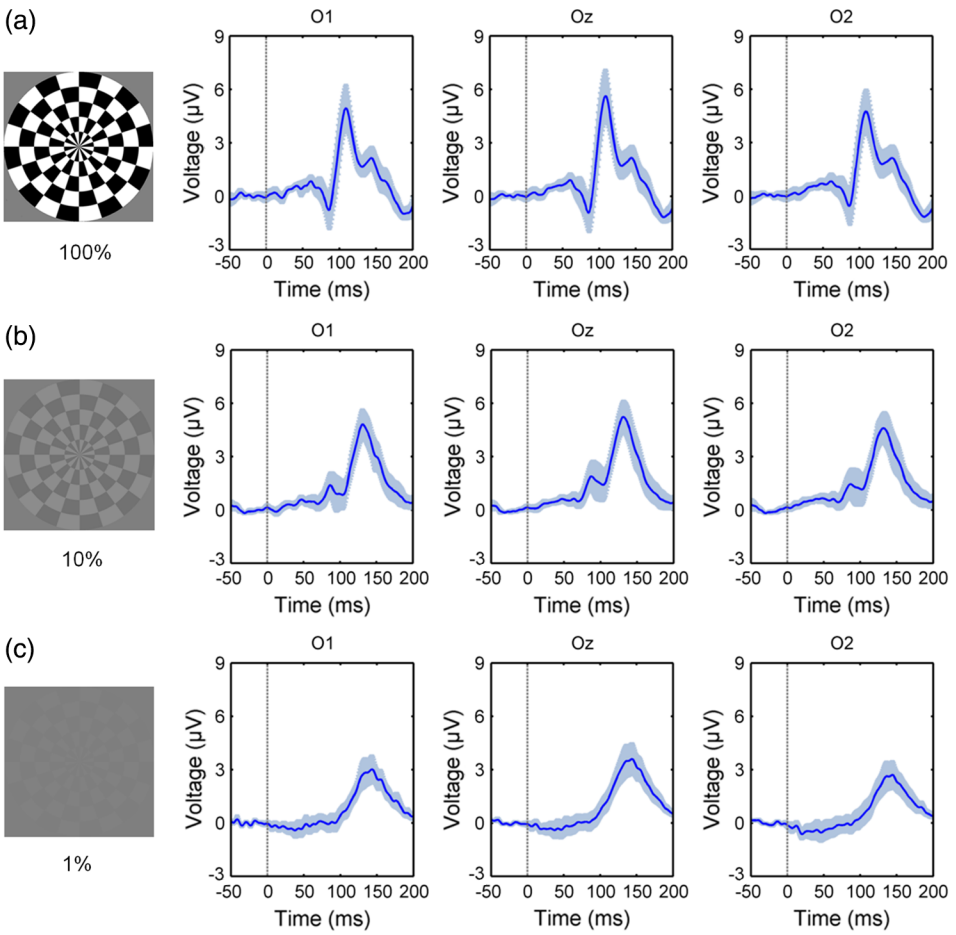

Fig. 2 The group-averaged VEP results for the visual checkerboard reversal tasks at different contrast levels: (a) 100%, (b) 10%, (c) 1%, recorded from electrodes O1, Oz, and O2. The shadow areas indicate the SE across the subjects. The gray lines represent the stimulus onset. For all three contrasts, the VEP amplitudes from channel Oz were relatively greater than those of channels O1 and O2, but the VEP latencies did not change significantly. In comparison, both the amplitude and latency of the VEPs varied with stimulus contrast, with the amplitude decreasing and the latency increasing as the stimulus contrast decreased.

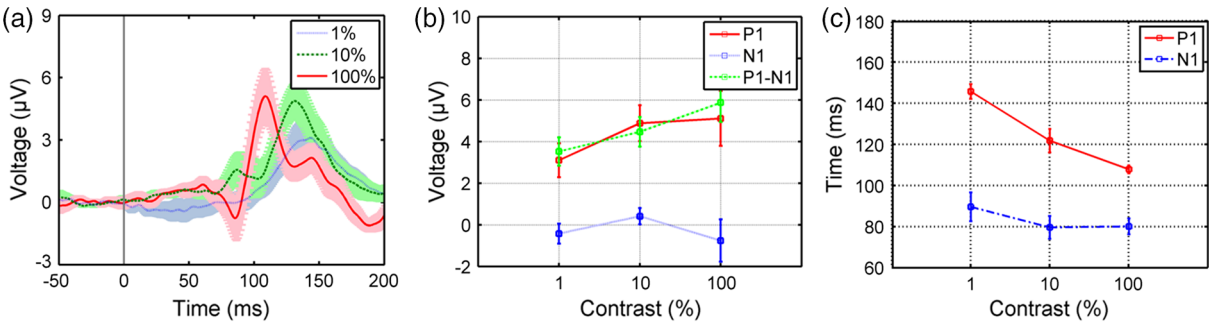

Fig. 3 The group-averaged mean VEPs across O1, Oz, and O2. (a) Comparison of VEPs across the 1%, 10%, and 100% contrasts, indicated in blue, green, and red curves, respectively. The shadow areas indicate the SE across the subjects. The gray line represents the stimulus onset. (b) The amplitudes of the VEPs against the stimulus contrast levels, error bars show the SE. (c) VEP latency responses to the various contrast levels, errors bars show the SE. The amplitudes of the mean VEPs increased monotonically, whereas the latencies decreased monotonically as the stimulus contrast increased.

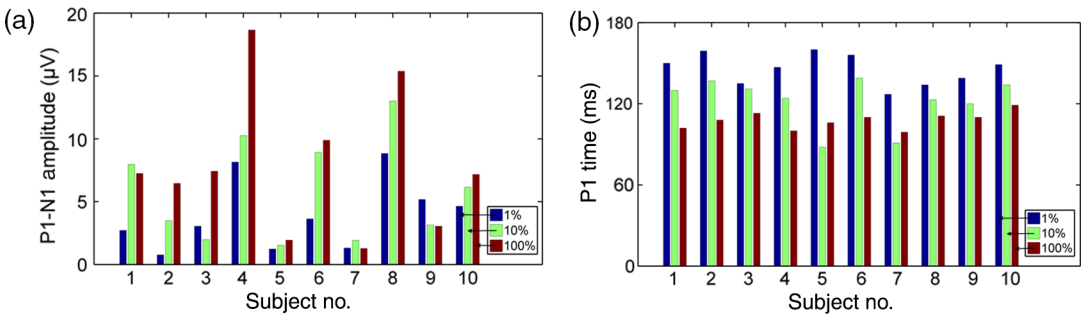

Fig. 4 VEP results for the visual checkerboard reversal tasks at different contrast levels by individual subject. (a) VEP amplitudes and (b) latencies for the different contrast levels for each subject. The blue (left column), green (middle column), and red (right column) bars represent 1%, 10%, and 100% contrast, respectively. The trends and magnitudes of the VEP amplitudes from contrast 1% to contrast 100% varied considerably between the subjects, but the VEP latencies showed much less inter-subject variability.

Table 1 Overview of the peak values and peak times of the VEP and the corresponding hemodynamic responses at three contrast levels (mean ± SE).

Contrast	Type	1%	10%	100%
HbO	Amplitude (μmol/l)	$0.138 \pm 0.02^{b,c}$	$0.246 \pm 0.05^{a,c}$	$0.318 \pm 0.042^{a,b}$
	Peak time (s)	19.96 ± 2.41	19 ± 3.15	18.06 ± 2.82
Hb	Amplitude (μmol/l)	-0.066 ± 0.007^{c}	-0.072 ± 0.021	-0.122 ± 0.014^{a}
	Peak time (s)	18.86 ± 2.81	20.02 ± 3.34	18.32 ± 2.78
P1-N1	Amplitude (μV)	$3.52 \pm 0.68^{b,c}$	$4.47 \pm 0.71^{a,c}$	$5.87 \pm 0.94^{a,b}$
P1	Amplitude (μV)	$3.09 \pm 0.81^{b,c}$	4.88 ± 0.86^{a}	5.11 ± 1.32^{a}
	Latency (ms)	$145.61 \pm 3.59^{b,c}$	$121.73 \pm 5.7^{a,c}$	$107.84 \pm 1.97^{a,b}$
N1	Amplitude (μV)	-0.43 ± 0.48^{b}	$0.41 \pm 0.39^{a,c}$	-0.76 ± 1.01^{b}
	Latency (ms)	89.64 ± 7.01	79.61 ± 5.49	80.15 ± 3.83

[a]Significant difference with contrast 1% at $p < 0.05$.
[b]Significant difference with contrast 10% at $p < 0.05$.
[c]Significant difference with contrast 100% at $p < 0.05$.

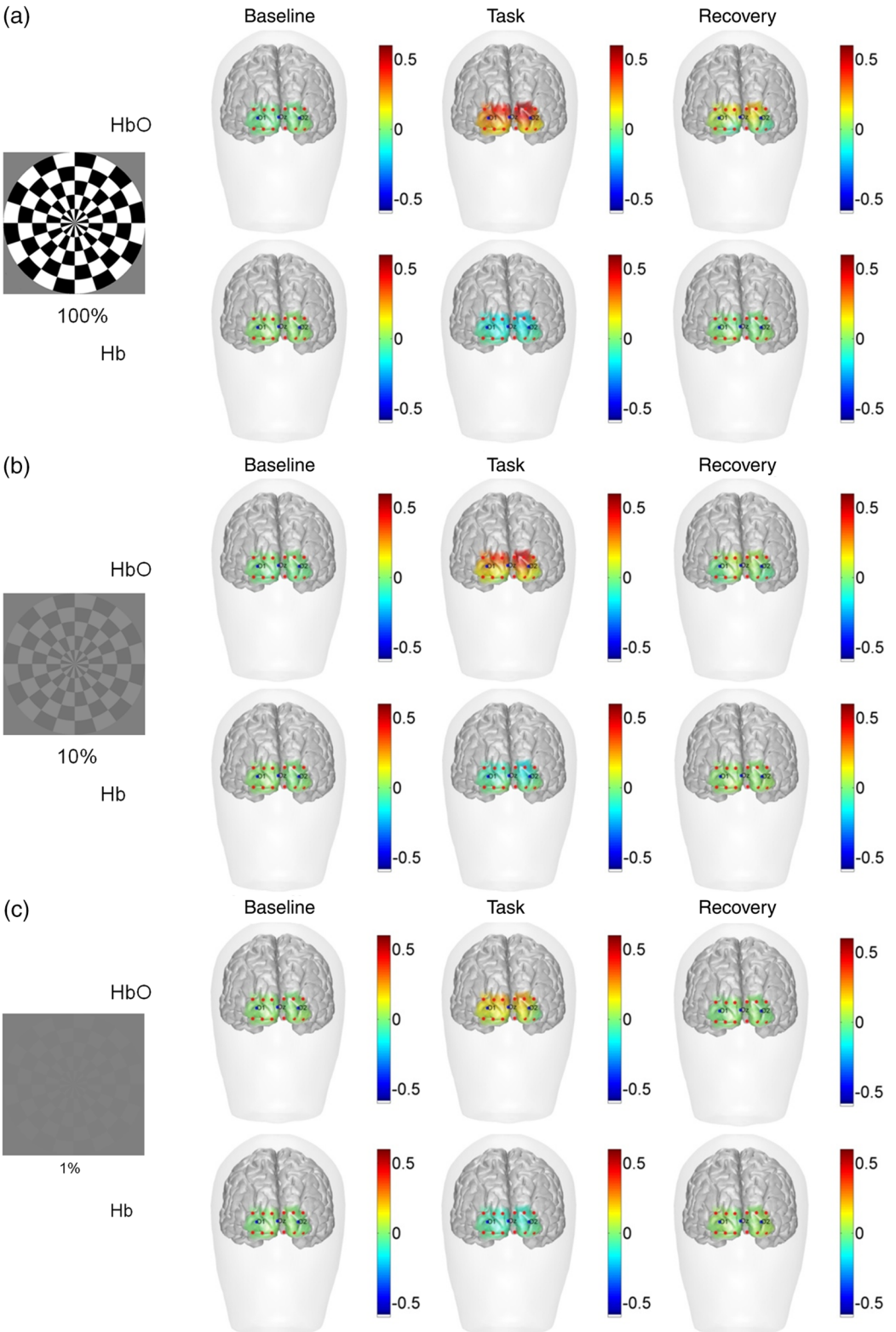

Fig. 5 The group-averaged spatial distribution maps of the hemodynamic responses for the visual checkerboard reversal tasks at different contrast levels: (a) 100%, (b) 10%, and (c) 1%, during the baseline (left column, $t = -5$ s), task (middle column, $t = 18$ s), and recovery (right column, $t = 40$ s) for HbO (top row) and Hb (bottom row) at each contrast level. The color bar indicates the ΔHbO or ΔHb in μmol/l.

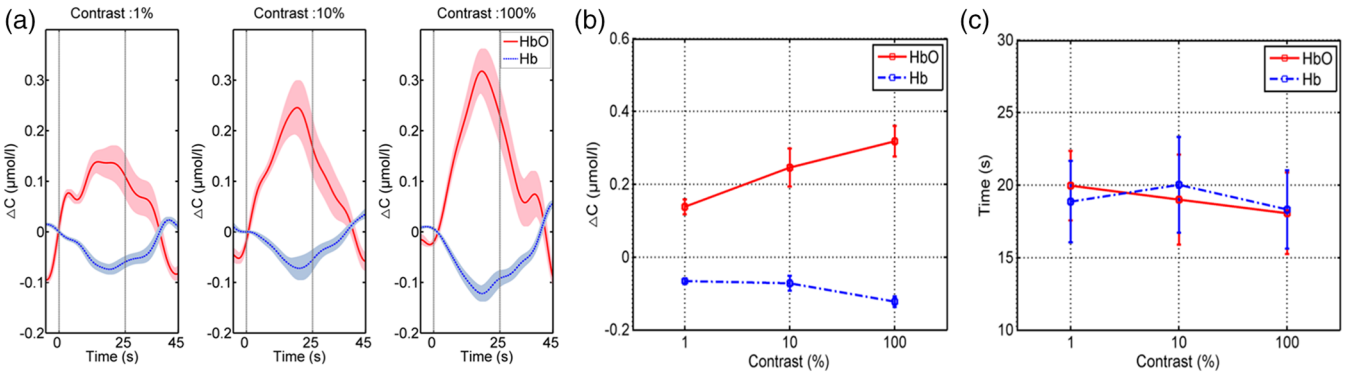

Fig. 6 The group-averaged mean hemodynamic responses across all channels. (a) Comparison of the hemodynamic responses across the 1%, 10%, and 100% contrast levels. The red and blue curves in all the graphs represent ΔHbO and ΔHb, respectively. The shadow areas indicate the SE. The stimulus duration is indicated by the space between the two gray lines. (b) and (c) show the amplitudes and the peak time of the hemodynamic response as a function of the stimulus contrast levels, respectively; error bars show the SE. The amplitudes of the ΔHbO monotonically increased as the contrast level increased, but increased more slowly at the high contrast level. However, the peak time of the ΔHbO monotonically decreased as the contrast level increased. Both the changes in the amplitudes and the peak time in the ΔHbO are more apparent than those in the ΔHb.

whereas the latencies of the VEPs showed low variability and high stability among the subjects.

3.2 *Functional Near Infrared Spectroscopy Results*

The group-averaged spatial distribution maps of the hemodynamic responses for the visual checkerboard reversal tasks at different contrast levels are shown in Fig. 5. Figure 6 shows the group-averaged mean hemodynamic responses across all the channels.

As is shown in Figs. 5 and 6, the hemodynamic responses from all three contrast levels showed significant increases in the amplitude of ΔHbO and decreases in the amplitude of ΔHb in response to neuronal activities. Moreover, the changes in ΔHbO are more apparent than those of ΔHb. Throughout the experiment, a poststimulus undershoot can be seen in several channels across the three contrast levels.

In comparison, the amplitudes of the ΔHbO increased as the contrast level increased, but seemingly may have increased more slowly at the highest contrast level. What is more, there were no obvious changes in the amplitudes of the ΔHb with varying contrast levels. Note that the peak time of the ΔHbO monotonically decreased as the contrast level increased. Both the changes in the amplitudes and the peak time in the ΔHbO were more apparent than those in the ΔHb. All three contrast levels were compared statistically with each other. As can be seen in Table 1, the amplitudes of ΔHbO at the three contrast levels were significantly different from each other (paired t-test, $p < 0.05$), but for ΔHb, only the 1% contrast was statistically different from the 100% contrast level. As for the peak time of the hemodynamic responses, neither the ΔHbO nor the ΔHb showed any significant differences between all three contrast levels, although a weak trend toward decreasing peak time with increasing contrast level was present in the ΔHbO.

3.3 *Correlation Results*

In this paper, we used the P1–N1 amplitude for the correlation analysis because it has a greater dynamic range than those of the P1 and N1 amplitudes alone.[50] For latency, the first positive P1 peaks were used for analysis because of their relatively good stability.[51,52] The correlation between the amplitude of VEP and hemodynamic responses at the different stimulus contrast levels is illustrated in Fig. 7(a), which seems to indicate a linear

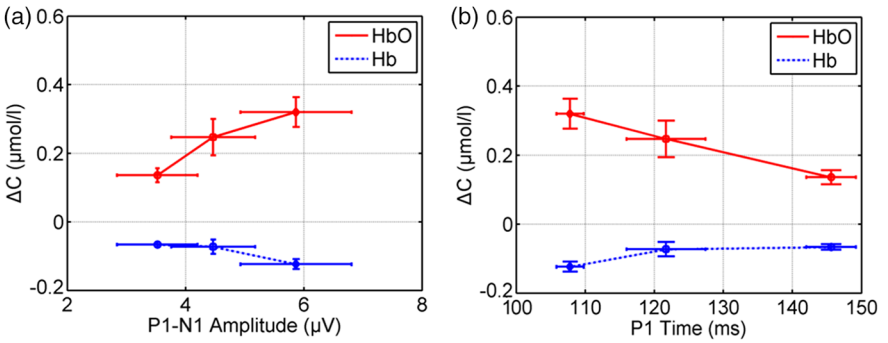

Fig. 7 The correlation between the VEP and hemodynamic responses at the different stimulus contrast levels. (a) and (b) indicate the relationship between VEP amplitude and latency against the hemodynamic response at the different contrast levels. The circle, square, and rhombus represent the 1%, 10%, and 100% contrast levels, respectively. The red and blue lines indicate the ΔHbO and the ΔHb, respectively. Error bars show the SE.

relationship between them. In contrast, decreases in the P1 latency were related to increases in the amplitude of the hemodynamic response, implying a negative relationship, see Fig. 7(b).

4 Discussion and Conclusions

Brain functional activity has been a hot topic in both neuroscience and clinical neurology. VEPs have frequently been used as psychophysiological signals in clinical situations and neuroscience studies. The amplitude characteristic of the VEP, which is the first of two key parameters of event-related potentials, has been associated with the hemodynamic response.[22–32] However, there have been relatively few studies investigating the relationship between the latency of the VEPs and the hemodynamic responses. Since brain activity involves a complicated chain reaction of cellular, metabolic, and vascular processes, it is impossible to rely on one neuroimaging modality to unveil the brain's complicated mechanisms. Moreover, involving two or more imaging modalities could provide complementary information about the activity. fNIRS and EEG are a natural pair in that they have compatible spatial and temporal resolution and can enrich each other with different types of physiological information. Therefore, in this study we utilized fNIRS and EEG as a multimodal neuroimaging method to analyze the relationship between neuronal activities and the hemodynamic responses. The main difference between the current work and previous studies is that not only the amplitude characteristics but also the temporal characteristics (specifically, the latencies of the VEPs and the peak time of the hemodynamic responses) of the neuronal activities and hemodynamic responses were also investigated.

The checkerboard reversal stimulus was used to evoke activity in the visual cortex. Neuronal electrophysiological signals and the vascular microcirculation were measured noninvasively by EEG and fNIRS, respectively. To quantify the relationship between the amplitude/latency and the hemodynamic response, the visual stimuli were presented at three contrast levels, 1%, 10%, and 100%. We analyzed the effects of the graded stimuli to the amplitude/latency and to the hemodynamic response, as well as the relationship between these two modalities.

4.1 *Neuronal Responses to Graded Stimulation*

VEPs have a typical waveform under visual stimuli with 100% contrast. Our VEPs at the 100% level were in line with previously published VEP waveforms obtained using the same task.[17,20,53] The amplitudes and latencies varied slightly from reports in other studies, possibly because of differences in the experimental protocols, such as check size, stimulus frequency, attention level, and age.[17] Moreover, the VEPs had relatively high variability between subjects in their amplitudes but low variability and high stability in their latencies. These results were in agreement with a previous study,[18] which claimed that the latency measurements tend to have less between-subject variation than the amplitudes.

Both the amplitude and the latency of VEP varied with the stimulus contrast level. The higher the contrast level of the stimulus, the greater the amplitude of the VEP. But the latency showed an opposite trend. The higher the contrast level of the stimulus, the shorter the latency. Our results are in agreement with previous research.[24,36,54,55] Interestingly, the rate of change in the amplitude was slower at the higher contrast level. This could have been due to a saturation effect.[24,56] A logarithmic function may be appropriate to represent VEP amplitudes at different contrasts.[25,55,56]

4.2 *Hemodynamic Responses to Graded Stimulation*

After the visual stimulation, the hemodynamic responses showed significant increases in the ΔHbO and decreases in the ΔHb with an increasing level of stimulus contrast. Moreover, the rate of increase in the ΔHbO was more apparent than the rate of decrease in the ΔHb. This may have been due to a relatively higher signal-to-noise ratio for ΔHbO, which could have improved its robustness to cross-talk.[46,57] These results were in accord with previous findings.[24,58] Typically, the rate of change of the hemodynamic response gradually decreased as the contrast increased. The relationship between the hemodynamic responses and contrast levels also follows a logarithmic function.[25,54,55] For a given stimulus, the recorded hemodynamic response is the mixed results of several complex processes, including the neuronal activity responding to the stimulus, the neurovascular coupling relationship between neuronal activity and the hemodynamic response, and the nature of the hemodynamic response itself.[59] Therefore, hemodynamic nonlinearity might result from any one or a mixture of these processes, rather than from the vascular effect alone.[24] In this paper, the consistency of the logarithmic changes in the VEPs and the hemodynamic responses in response to visual contrasts may indicate that the hemodynamic nonlinearity primarily reflects the nonlinearity of underlying neuronal activity.[24]

4.3 *Neurovascular Coupling Function*

VEPs are induced by the summation of synchronous neuronal activities of similarly aligned neurons and are typically sensitive to the conductive properties of the brain. VEPs can be cancelled out by opposing current sources under certain conditions.[29,33] Hemodynamic responses result from the integration of the synaptic inputs of the entire neuronal population of a region of interest regardless of the orientation or the excitatory or inhibitory role of those neurons.[29] A high contrast stimulus, such as our 100% contrast level, represents a "strong stimulus", which should be expected to take less time for the neurons to become synchronized and should produce a higher amplitude of responses in the visual cortex.

The hemodynamic response is thought to be a low-pass filter of the underlying neural activity.[4] This means that the hemodynamic response integrates both the spatial and temporal information of the neural activity.[24] In order to investigate the visual evoked functional activity comprehensively, we examined the correlation between the hemodynamic changes and the amplitude and latency of the VEP. Our study showed that, with an increase in visual contrast, both the amplitude of the evoked potentials and the hemodynamic responses increased correspondingly, implying a linear relationship between them. This agrees with previous studies.[23,25] Typically, according to Koch et al.,[15] a logarithmic increase in contrast levels results in a linear correlation between the neuronal (both the transient VEP and the gamma band activity) and hemodynamic responses.

However, the latency of the VEP decreased when the stimulus contrast increased. This finding implies a negative correlation between the VEP latency and the hemodynamic responses. A possible physiological mechanism is that the decreased

response latency of the VEP could be related to a larger amplitude of the hemodynamic response because neurons become synchronized more rapidly in response to a strong stimulus, resulting in a shorter response latency. Moreover, it is well established that neuronal activity consumes energy. More energy is required for neurons to generate action potentials in a shorter time leading to stronger hemodynamic responses. This mechanism does not conflict with the conventional strength mechanism by which an increase in the response amplitude of the VEP is associated with a larger amplitude of the hemodynamic response. What is more important about this mechanism based on latency is that it illustrates another possible way that the time relationship can provide supplementary information that may increase the understanding and interpretation of the relationship between electrical activities and hemodynamic responses.

4.4 *Limitations of the Current Study*

One of the limitations of the current study is that only three contrast levels were used. Future studies using more contrast levels would be helpful for addressing the relationship between neural and hemodynamic responses in greater detail. A second limitation is the relatively low spatial resolution. Employing high-density EEG and high-density tomography at multiple distances will be helpful for understanding the neurovascular coupling mechanism in greater detail. In that way the task irrelevant noises of the fNIRS that result from shallow tissue (scalp and skin) could be further eliminated or at least reduced and the spatial resolution could be improved. An additional limitation is that the EEG and fNIRS measurements were recorded separately. Therefore, the exact experimental configuration and attention level could have been different. In further studies, simultaneous recording might be helpful for overcoming this limitation.

Acknowledgments

We appreciate the assistance that Rhoda and Edmund Perozzi, PhDs, provided in proofreading and critiquing this work. This work was partially supported by the National Key Scientific Instrument and Equipment Development Project of China (2012YQ120046) and the Natural Science Foundation of China (Grant No. 31571003).

References

1. D. Attwell and C. Iadecola, "The neural basis of functional brain imaging signals," *Trends Neurosci.* **25**(12), 621–625 (2002).
2. G. Strangman, D. A. Boas, and J. P. Sutton, "Non-invasive neuroimaging using near-infrared light," *Biol. Psychiatry* **52**(7), 679–693 (2002).
3. R. J. Cooper, *Development of Simultaneous Electroencephalography and Near-infrared Optical Topography for Applications to Neurovascular Coupling and Neonatal Seizures*, University College London (2010).
4. N. K. Logothetis and J. Pfeuffer, "On the nature of the BOLD fMRI contrast mechanism," *Magn. Reson. Imaging* **22**(10), 1517–1531 (2004).
5. B. Yesilyurt et al., "Relationship of the BOLD signal with VEP for ultra-short duration visual stimuli (0.1 to 5 ms) in humans," *J. Cereb. Blood Flow Metab.* **30**(2), 449–458 (2010).
6. H. Laufs et al., "EEG-correlated fMRI of human alpha activity," *Neuroimage* **19**(4), 1463–1476 (2003).
7. A. Salek-Haddadi et al., "Hemodynamic correlates of epileptiform discharges: an EEG-fMRI study of 63 patients with focal epilepsy," *Brain Res.* **1088**(1), 148–166 (2006).
8. C. Benar et al., "Quality of EEG in simultaneous EEG-fMRI for epilepsy," *Clin. Neurophysiol.* **114**(3), 569–580 (2003).
9. F. F. Jobsis, "Noninvasive, infrared monitoring of cerebral and myocardial oxygen sufficiency and circulatory parameters," *Science* **198**(4323), 1264–1267 (1977).
10. S. Fazli et al., "Enhanced performance by a hybrid NIRS-EEG brain computer interface," *Neuroimage* **59**(1), 519–529 (2012).
11. M. Ferrari and V. Quaresima, "A brief review on the history of human functional near-infrared spectroscopy (fNIRS) development and fields of application," *Neuroimage* **63**(2), 921–935 (2012).
12. B. W. Zeff et al., "Retinotopic mapping of adult human visual cortex with high-density diffuse optical tomography," *Proc. Natl. Acad. Sci. U. S. A.* **104**(29), 12169–12174 (2007).
13. B. Koo et al., "A hybrid NIRS-EEG system for self-paced brain computer interface with online motor imagery," *J. Neurosci. Methods* **244**, 26–32 (2015).
14. N. Roche-Labarbe et al., "NIRS-measured oxy- and deoxyhemoglobin changes associated with EEG spike-and-wave discharges in children," *Epilepsia* **49**(11), 1871–1880 (2008).
15. S. P. Koch et al., "Stimulus-induced and state-dependent sustained gamma activity is tightly coupled to the hemodynamic response in humans," *J. Neurosci.* **29**(44), 13962–13970 (2009).
16. F. Wallois et al., "Usefulness of simultaneous EEG-NIRS recording in language studies," *Brain Lang.* **121**(2), 110–123 (2012).
17. J. V. Odom et al., "ISCEV standard for clinical visual evoked potentials (2009 update)," *Doc. Ophthalmol.* **120**(1), 111–119 (2010).
18. Diopsys, "The ABCs of VEP office based visual evoked potential: descriptions, methods and applications," in *Office based Visual Evoked Potential*, 2nd ed. (2013).
19. A. M. Norcia and C. W. Tyler, "Spatial frequency sweep VEP: visual acuity during the first year of life," *Vision Res.* **25**(10), 1399–1408 (1985).
20. P. Walsh, N. Kane, and S. Butler, "The clinical role of evoked potentials," *J. Neurol. Neurosurg. Psychiatry* **76**(Suppl 2), ii16–ii22 (2005).
21. S. Tobimatsu and G. G. Celesia, "Studies of human visual pathophysiology with visual evoked potentials," *Clin. Neurophysiol.* **117**(7), 1414–1433 (2006).
22. K. Kashikura et al., "Temporal characteristics of event-related BOLD response and visual-evoked potentials from checkerboard stimulation of human V1: a comparison between different control features," *Magn. Reson. Med.* **45**(2), 212–216 (2001).
23. H. Obrig et al., "Habituation of the visually evoked potential and its vascular response: implications for neurovascular coupling in the healthy adult," *Neuroimage* **17**(1), 1–18 (2002).
24. X. Wan et al., "The neural basis of the hemodynamic response nonlinearity in human primary visual cortex: Implications for neurovascular coupling mechanism," *Neuroimage* **32**(2), 616–625 (2006).
25. L. Rovati et al., "Optical and electrical recording of neural activity evoked by graded contrast visual stimulus," *Biomed. Eng. Online* **6**, 28 (2007).
26. N. Zhang et al., "Noninvasive study of neurovascular coupling during graded neuronal suppression," *J. Cereb. Blood Flow Metab.* **28**(2), 280–290 (2008).
27. J. A. de Zwart et al., "Hemodynamic nonlinearities affect BOLD fMRI response timing and amplitude," *Neuroimage* **47**(4), 1649–1658 (2009).
28. Z. Liu et al., "Linear and nonlinear relationships between visual stimuli, EEG and BOLD fMRI signals," *Neuroimage* **50**(3), 1054–1066 (2010).
29. S. D. Mayhew et al., "Coupling of simultaneously acquired electrophysiological and haemodynamic responses during visual stimulation," *Magn. Reson. Imaging* **28**(8), 1066–1077 (2010).
30. S. P. Koch et al., "Individual alpha-frequency correlates with amplitude of visual evoked potential and hemodynamic response," *Neuroimage* **41**(2), 233–242 (2008).
31. T. Zaehle et al., "Inter- and intra-individual covariations of hemodynamic and oscillatory gamma responses in the human cortex," *Front. Human Neurosci.* **3**, 8 (2009).
32. S. P. Koch et al., "Synchronization between background activity and visually evoked potential is not mirrored by focal hyperoxygenation: implications for the interpretation of vascular brain imaging," *J. Neurosci.* **26**(18), 4940–4948 (2006).
33. Y. Kaneoke, "Magnetoencephalography: In search of neural processes for visual motion information," *Progr. Neurobiol.* **80**(5), 219–240 (2006).

34. K. Whittingstall et al., "Correspondence of visual evoked potentials with FMRI signals in human visual cortex," *Brain Topogr.* **21**(2), 147–147 (2008).
35. J. H. Maunsell et al., "Visual response latencies of magnocellular and parvocellular LGN neurons in macaque monkeys," *Vis. Neurosci.* **16**(1), 1–14 (1999).
36. A. Vassilev, M. Mihaylova, and C. Bonnet, "On the delay in processing high spatial frequency visual information: reaction time and VEP latency study of the effect of local intensity of stimulation," *Vision Res.* **42**(7), 851–864 (2002).
37. M. W. Oram, "Contrast induced changes in response latency depend on stimulus specificity," *J. Physiol. Paris* **104**(3–4), 167–175 (2010).
38. J. F. Connolly and J. H. Gruzelier, "Amplitude and latency changes in the visual evoked potential to different stimulus intensities," *Psychophysiology* **19**(6), 599–608 (1982).
39. T. J. Gawne, T. W. Kjaer, and B. J. Richmond, "Latency: another potential code for feature binding in striate cortex," *J. Neurophysiol.* **76**(2), 1356–1360 (1996).
40. D. S. Reich, F. Mechler, and J. D. Victor, "Temporal coding of contrast in primary visual cortex: when, what, and why," *J. Neurophysiol.* **85**(3), 1039–1050 (2001).
41. B. Ozus et al., "Rate dependence of human visual cortical response due to brief stimulation: an event-related fMRI study," *Magn. Reson. Imaging* **19**(1), 21–25 (2001).
42. C. H. Chen et al., "A noninvasive brain computer interface using visually-induced near-infrared spectroscopy responses," *Neurosci. Lett.* **580**, 22–26 (2014).
43. A. Bozkurt et al., "A portable near infrared spectroscopy system for bedside monitoring of newborn brain," *Biomed. Eng. Online* **4**, 29 (2005).
44. L. Kocsis, P. Herman, and A. Eke, "The modified Beer–Lambert law revisited," *Phys. Med. Biol.* **51**(5), N91–N98 (2006).
45. X. Cui, S. Bray, and A. L. Reiss, "Functional near infrared spectroscopy (NIRS) signal improvement based on negative correlation between oxygenated and deoxygenated hemoglobin dynamics," *Neuroimage* **49**(4), 3039–3046 (2010).
46. S. K. Piper et al., "A wearable multi-channel fNIRS system for brain imaging in freely moving subjects," *Neuroimage* **85**(Pt 1), 64–71 (2014).
47. A. Duncan et al., "Measurement of cranial optical path length as a function of age using phase resolved near infrared spectroscopy," *Pediatr. Res.* **39**(5), 889–894 (1996).
48. M. A. Franceschini et al., "Hemodynamic evoked response of the sensorimotor cortex measured noninvasively with near-infrared optical imaging," *Psychophysiology* **40**(4), 548–560 (2003).
49. K. L. Koenraadt et al., "Multi-channel NIRS of the primary motor cortex to discriminate hand from foot activity," *J. Neural Eng.* **9**(4), 046010 (2012).
50. D. Fuglo et al., "Correlation between single-trial visual evoked potentials and the blood oxygenation level dependent response in simultaneously recorded electroencephalography-functional magnetic resonance imaging," *Magn. Reson. Med.* **68**(1), 252–260 (2012).
51. K. Kunita and K. Fujiwara, "Changes in the P100 latency of the visual evoked potential and the saccadic reaction time during isometric contraction of the shoulder girdle elevators," *Eur. J. Appl. Physiol.* **92**(4–5), 421–424 (2004).
52. J. Zhao, S. Pang, and G. Che, "Specificity and sensitivity of visual evoked potentials P100 latency to different events exercise," *Health* **1**, 47–50 (2009).
53. B. Sun et al., "Detection of optical neuronal signals in the visual cortex using continuous wave near-infrared spectroscopy," *Neuroimage* **87**, 190–198 (2014).
54. M. Zaletel et al., "The relationship between visually evoked cerebral blood flow velocity responses and visual-evoked potentials," *Neuroimage* **22**(4), 1784–1789 (2004).
55. J. Schadow et al., "Stimulus intensity affects early sensory processing: visual contrast modulates evoked gamma-band activity in human EEG," *Int. J. Psychophysiol.* **66**(1), 28–36 (2007).
56. G. S. Souza et al., "Contrast sensitivity of pattern transient VEP components: contribution from M and P pathways," *Psychol. Neurosci.* **6**, 191–198 (2013).
57. G. Strangman, M. A. Franceschini, and D. A. Boas, "Factors affecting the accuracy of near-infrared spectroscopy concentration calculations for focal changes in oxygenation parameters," *Neuroimage* **18**(4), 865–879 (2003).
58. C. L. Liang et al., "Luminance contrast of a visual stimulus modulates the BOLD response more than the cerebral blood flow response in the human brain," *Neuroimage* **64**, 104–111 (2013).
59. O. J. Arthurs and S. Boniface, "How well do we understand the neural origins of the fMRI BOLD signal?," *Trends Neurosci.* **25**(1), 27–31 (2002).

Juanning Si is a PhD candidate at the Institute of Automation, Chinese Academy of Sciences. She received her BS and MS degrees in Control Theory and Control Engineering from the North China Electric Power University in 2008 and 2011, respectively. Her current research interests include applications of fNIRS and EEG and neurovascular coupling analysis. She is a member of SPIE.

Xin Zhang is an associate professor at the Institute of Automation, Chinese Academy of Sciences. He received his BS and MS degrees in biomedical engineering from the Capital Medical University in 2002 and Tsinghua University in 2006, respectively, and his PhD degree in electric and electronic engineering from the University of Hong Kong in 2010. His research interests include neurophotonics and neurohemodynamics. He is a member of SPIE.

Yuejun Li is a PhD candidate at the School of Life Science and Technology, University of Electronic Science and Technology of China. He received his BS degree in computers and applications from the Henan University of Science and Technology of China in 2008 and MS degree in computer application technology from the Henan Normal University of China in 2012, respectively. His current research interests center around statistical analysis of MEG data in patients with epilepsy.

Yujin Zhang is an assistant professor at the Institute of Automation, Chinese Academy of Sciences. She received her BS degree in communication engineering from Tianjin University in 2007, and her PhD degree in cognitive neuroscience from Beijing Normal University in 2013. Her research interests include spontaneous brain activations during resting state, data analysis and clinical applications of functional near infrared spectroscopy, and simultaneous electrophyiological and functional near infrared spectroscopy recordings.

Nianming Zuo is an associate professor at the Institute of Automation, Chinese Academy of Sciences (CASIA). He received his BS in mathematics from Shandong University in 2002 and PhD in medical imaging in Chinese Academy of Sciences in 2007, respectively. Before joining the Brainnetome Center, CASIA, he was a research scientist in Kodak Health Group in Shanghai, China. His current research interests include medical image processing and brain imaging neuroscience.

Tianzi Jiang is professor of neuroimaging and brain disorders at Institute Automation of the Chinese Academy of Sciences (CASIA), and professor of Queensland Brain Institute, University of Queensland. He is director of Brainnetome Center of CASIA. His research interests include neuroimaging, brainnetome, imaging genetics, and their clinical applications in brain disorders. He is the author over 200 reviewed journal papers in these fields. He is associate editor of a number of journals in these fields.